Movement of fluids in the Nankai Trough area: Insights from ^{129}I and halogen distributions along the IODP NanTroSEIZE transect

Hitoshi Tomaru[1]*, Udo Fehn[2]

[1]Department of Earth Sciences, Chiba University, Chiba 263-8522, Japan

[2]Department of Earth and Environmental Sciences, University of Rochester, Rochester, NY 14627, USA

*Corresponding author

Phone: +81-43-290-2862

Fax: +81-43-290-2862

E-mail: tomaru@chiba-u.jp

ABSTRACT

Halogen concentrations and $^{129}I/I$ ratios were determined in pore waters from the Nankai Trough subduction system, collected during IODP Expeditions 315, 316, 322, and 333 along the NanTroSEIZE transect. The transect allowed the first direct comparison of iodine results across an active subduction system, from subducting oceanic sediments to the accretionary prism, and the overlying forearc basin. In contrast to the other halogens (Cl and Br) iodine concentrations show large variations within and among the cores at all sites landward of the trough, I concentrations increase rapidly with depth and reach values several orders of magnitude higher than those in seawater, but are only slightly higher than seawater values at the seaward sites. Methane concentrations follow a similar pattern. Host sediments of the fluids are younger than 7 Ma in all the cores, but the ages of iodine in pore waters at the landward sites reach values beyond 30 Ma., In contrast, iodine seaward of the trough is in isotopic equilibrium with the host sediments, resulting in very similar iodine and sediment ages. The distribution of iodine concentrations and ages indicates that iodine at the landward sites has been transported there in aqueous fluids, probably together with methane, from old formations in the upper plate. The specific fluid pathways potentially were influenced by features such as the megasplay fault in the prism or the decollement. The results demonstrate large-scale transport of fluids carrying iodine and other compounds such as methane from old layers in the upper plate to surface locations landward of the Nankai Trough, while separate, but only local hydrologic processes occur in the marine sediments moving toward the trough.

Key words: NanTroSEIZE, Nankai Trough, pore water, iodine, ^{129}I

1. INTRODUCTION

Integrated Ocean Drilling Program (IODP) Expeditions 315, 316, 322, and 333 were carried out from 2007 to 2011 by D/V *Chikyu* as parts of the multistage Nankai Trough Seismogenic Zone Experiment (NanTroSEIZE). During these expeditions, the Kumano Forearc Basin sediment was cored down to the upper accretionary prism as well as the accretionary prism itself including brecciated/fractured, deformed zones associated with subduction processes and earthquakes (Fig. 1). The inputting hemipelagic/pelagic Shikoku Basin sediments on the subducting Philippine Sea Plate were also cored to the uppermost igneous basement along the NNW-SSE transect in the Nankai Trough, Japan. This program has provided numerous scientific resources to construct entire geological processes induced by plate subduction covering the loci of future input to the past accretion of sediments. We have focused on the behavior of fluids filling sediment pores, indicative of material remobilization, because marine pore water is a medium that captures and conveys materials originated from minerals and seawater due to sedimentation and accretion. The geochronology of a long-lived radioisotope of iodine (^{129}I) has shown to be useful for the identification of sources and migration paths for sedimentary fluids, particularly on continental margins (Fehn et al., 2000, 2007a; Fehn, 2012). Here we examine pore water regimes with iodine geochronology including major accretionary processes, lithology change, fault/thrust activity, and subducting/inputting, across the Nankai Trough seismogenic zone. This approach allows the investigation of changes in iodine and methane concentrations across an active margin and of their relation to fluid flow in a subduction zone. In addition, the comparison between iodine concentrations and ^{129}I/I ratios on both sides of the Nankai Trough provides insights into the systematics of this isotopic

system in coastal areas and the open ocean.

2. IODINE GEOCHRONOLOGY

Applications of the iodine isotopic system are based on the presence of the radioisotope, ^{129}I, which allows dating with a range of 100 Ma. Iodine is strongly associated with organic materials such as phytoplankton and algae in marine environments, where it can reach concentrations up to 10,000 ppm. Consequently, marine sediments constitute the major iodine reservoir in the earth's surface (Elderfield and Truesdale, 1980; Harvey, 1980; Muramatsu and Wedepohl, 1998). After sedimentation and burial of organic-rich sediments, iodine typically is released into aqueous phases during the decomposition of organic particulates, but a large fraction of that iodine is returned back into the overlying seawater (Ullman and Aller, 1980, 1983). Iodine concentrations in pore waters are higher than those in seawater of 0.05 ppm or 0.44 μM (e.g., Fuge and Johnson, 1986) and range mostly between 1 and 10 ppm (e.g., Kennedy and Elderfield, 1987). Exceptions are situations with the strong presence of methane in fluids, such as gas hydrate occurrences, where iodine concentrations can reach values as high as 250 ppm or 2 mM (e.g., Martin et al., 1993; Egeberg and Dickens, 1999; Fehn et al., 2006).

Iodine has one stable isotope (^{127}I) and one long-lived radioisotope (^{129}I) with a half-life of 15.7 Myr, which is produced by the spontaneous fission of ^{238}U in the crust or sediment and cosmic ray spallation of Xe isotopes in the atmosphere. Because of constant and similar contribution of ^{129}I from these two sources into the marine iodine system and the relatively long residence time of iodine in seawater (~300 kyr; Broecker and Peng, 1982), compared with that in the atmosphere (~14 days), and with the

turn-over time of seawater (~1,000 yr), the isotopic ratio of ^{129}I to total iodine (^{129}I/I) among surface reservoirs can be assumed to be homogeneous. The ^{129}I/I ratio in the surface reservoirs has, however, been increased by several orders of magnitude since the beginning of the nuclear age due to the release of ^{129}I from anthropogenic activities, (Moran et al., 1999; Rao and Fehn, 1999; Santschi and Schwehr 2004; Snyder et al., 2010). The natural or pre-anthropogenic ratio for ^{129}I/I in surface reservoirs, has been determined to be $(1500\pm150)\times10^{-15}$ (Moran et al., 1998; Fehn et al., 2007b).

Dating using the ^{129}I system is based on the separation of iodine from the ocean at time *t* and is governed by the decay equation:

$$R_{obs}=R_i e^{-\lambda t} \quad (1)$$

where R_{obs} is the observed ^{129}I/I ratio, R_i the initial seawater ^{129}I/I ratio (1500×10^{-15}) and λ the decay constant of ^{129}I (4.41×10^{-8} y^{-1}). Potential additions of ^{129}I from the spontaneous fission of ^{238}U and of anthropogenic ^{129}I are not taken into consideration here, making the measured ratio a maximum value and the calculated age a minimum value for a given sample. The relatively low uranium content in sediments of the research area, <1 ppm (Plank and Langmuir, 1998), make contributions of fissiogenic ^{129}I unlikely, and anthropogenic ^{129}I has not been detected beyond the layer of bioturbation in marine sediments (Fehn et al., 1986; Moran et al., 1998). The iodine system has been useful for the determination and correlation of ages or source formations for iodine and implications for fluid flow (Fehn et al., 1992; Tomaru et al., 2007a, 2007b; Lu et al., 2008; Fehn, 2012).

3. GEOLOGICAL SETTINGS

The Nankai Trough was formed by the subduction of the Philippine Sea Plate under the

Eurasian Plate at a rate of ~4 to 6 cm/yr with an interface dipping of 3° to 7° (Fig. 1) (Seno et al., 1993; Kodaira et al., 2000; Heki and Miyazaki, 2001; Park et al., 2002; DeMets et al., 2010). The subducting Philippine Sea Plate along the NanTroSEIZE transect carries the incoming sediments of Shikoku Basin towards the trough, which constitute a relatively thin sediment package with ages ranging from 0 to 21 Ma (Jarrard, 1986). On the landward side of the trough, the accretionary prism is formed by the accreted and forearc basin sediments. While sediments in these formations sampled during this study range between 0 and 7 Ma (Kinoshita et al., 2009; Saito et al., 2010; Henry et al., 2012; Hayashi et al., 2011; Su, 2012), ages at depth are considerably older, related to the prior subduction configuration between Eurasian and Pacific Plates. Gas hydrates are ubiquitous in the Nankai Trough area and were the focus of two earlier investigations at several locations ~100 km to the NE of the present study (Fig. 1B) (Fehn et al., 2003; Tomaru et al., 2007a). Although gas hydrates were observed also in several of the cores discussed here, they occurred only in those on the landward side of the trough. A large out-of-sequence thrust/fault system branching from the plate interface has been found in seismic profiles and a laterally extensive major fault, the megasplay fault (Fig. 1D), is identified distinctly in the research area (Park et al., 2002; Conin et al., 2012).

During IODP Expedition 315, we cored the upper accretionary prism at two sites; Site C0001 at the seaward edge of the Kumano Basin uplift (outer arc high) on the hanging wall of the megasplay fault, and Site C0002 at the southern margin of the basin (Fig. 1) (Kinoshita et al., 2009). Holocene to late Pliocene silty clay to clayey silt with intercalations of volcanic ash is unconformably underlain by the upper accretionary prism of late Miocene age composed mainly of mudstone, which are bounded by a thick

sand layer at 207 m core depth below seafloor (CSF) at Site C0001. An unconformity between the forearc basin and accretionary prism is identified by the lithology change from the basal Pliocene mudstone above to late Miocene interbeds of mudstone to sandstone below 922 m CSF at Site C0002. Logging-while-drilling (LWD) during Expedition 314 delineated these unit boundaries, and identified the accumulation of gas hydrates in sandy layers in the upper ~400 m CSF, but only at Site C0002.

During IODP Expedition 316, we cored the seaward edge of the Kumano Basin uplift where the megasplay fault is branching from the plate interface between the subducting Philippine Sea Plate and overlying Eurasian Plate at Site C0004. A 6 cm thick microbreccia, indicating concentrated shear within the megasplay fault zone, was found in the middle Pliocene hemipelagic section at 291 m CSF. Site C0008 is located ~1 km seaward of Site C0004, providing a reference site for the sediments underthrusting beneath the megasplay fault (Kinoshita et al., 2009). Onboard pore water analyses found accumulation of gas hydrate in some coarse layers between 70 and 170 m CSF at Site C0008 whereas no geochemical signs of gas hydrate occur at Site C0004. During IODP Expedition 333, Site C0018 was cored on a small slope basin seaward of the megasplay fault, ~5 km south-southwest of Site C0008. Holocene to Pleistocene hemipelagic clay is often interbedded there with volcanic ash layers and mass transport deposits above 191 m CSF, and sandy turbidites slope basin sediment down to 314 m CSF (Henry et al., 2012).

Sites C0006 and C0007, located at the main frontal thrust at the seaward edge of the accretionary wedge, were also cored during IODP Expedition 316 (Kinoshita et al., 2009). Late Miocene to middle Pleistocene mud is interbedded with volcanic ash and sand/silt layers, which were deposited in a trough setting. The uppermost section,

~30 m CSF, at these sites are composed of hemipelagic silty clay to silty sand with interbedded sands deposited on the lowermost slope above the trough floor. At Site C0006, cores are often tectonically brecciated/fractured between 230 and 545 m CSF. At Site C0007, fault zones were recognized between 238 and 259 m CSF, and 342 and 362 m CSF.

During IODP Expeditions 322 and 333, Sites C0011 and C0012 were investigated on the seaward side of the Trough. Site C0011 cored the Shikoku Basin sediments reaching almost the igneous basement on the subducting Philippine Sea Plate, which was formed by the backarc spreading of the Izu-Bonin volcanic arc during the early and middle Miocene (Okino et al., 1994; Kobayashi et al., 1995). The upper Shikoku Basin is composed of hemipelagic mud with abundant ash and volcaniclastic layers, underlain by middle Shikoku Basin hemipelagites with tuffaceous sandstone and volcaniclastic sand layers and lower Shikoku Basin bioturbated hemipelagites and turbidites (Saito et al., 2010; Henry et al., 2012). Middle Miocene tuffaceous silty claystone with zeolite and smectite from alteration of volcanic glass occurs from 850 m CSF. Log-seismic integration indicates a depth to igneous basement of ~1050 m below seafloor (Saito et al., 2010). Site C0012 is located on the basement high in the Shikoku Basin, which is composed of hemipelagic mud intercalated with volcanic ash/tuff, volcanoclastic sand, and siltstone layers similar to Site C0011. The basalt basement older than 18.9 Ma occurs at 538 m CSF, which is highly altered (Saito et al., 2010).

4. ANALYTICAL METHODS

For all the samples used here, a whole-round core of several tens of centimeter length was sectioned soon after core recovery and scraped in a nitrogen-filled glove bag

to avoid potentially contaminated surface sediments. The core section was then squeezed with a shipboard hydraulic press to extract pore water through 0.45 μm filters. Sample sizes ranged between 3 and 10 mL of pore waters. The sample aliquot was diluted by factors between 500 and 1000 with 5 wt% tetramethyl ammonium hydroxide solution for the determination of total dissolved iodine concentration and measured by inductively coupled plasma mass spectrometry (ICP-MS), HP4500 (Hewlett Packard/Agilent), at the University of Tokyo, with a standard deviation better than 3%.

For the measurement of $^{129}I/I$ ratio, silver iodide (AgI) was precipitated from the pore water samples at the Cosmogenic Isotope Lab, University of Rochester for samples from Sites C0001 to C0008 and at the University of Tokyo for samples from the other sites by established methods (Fehn et al., 1992). The sample solutions were oxidized to iodine with 30% hydrogen peroxide and nitric acid and then extracted into chloroform, back extracted into sodium bisulfite as iodide, and precipitated as AgI with 1 M silver nitrate. The AgI targets produced by these procedures were analyzed at the accelerator mass spectrometry (AMS) facility at PRIME Lab, Purdue University (Sharma et al., 2000). Because a minimum of 0.1 mg of I is required for reliable $^{129}I/I$ analyses (Lu et al., 2007), we had to combine between 3 and 9 neighboring samples to produce an AMS target. The weighted average depth and I concentration of $^{129}I/I$ samples were calculated from I concentrations and volumes of sample aliquots combined for AgI precipitation (Table 1). Error margins for depth in the $^{129}I/I$ profiles reflect the interval between the shallowest and deepest aliquots.

5. RESULTS

5.1. General properties of sediment and pore water

While iodine concentrations and isotopic ratios are the focus of this investigation, shipboard determinations of other parameters of sediments and pore waters are reported here together with the biostratigraphic age of cored sediments in order to put the iodine results into a wider context (Fig. 2). These results include sediment porosity calculated using the moisture and density (MAD) method in order to discuss potential movement of gases and pore waters. Determination of total organic carbon (TOC) in sediments and methane concentration in headspace samples and concentrations of other halogens (chlorine and bromine) are also reported. These data were collected onboard following the IODP standard protocol during the expeditions and are available on the respective IODP proceedings for these expeditions (Kinoshita et al., 2009; Saito et al., 2010; Henry et al., 2012).

The TOC values decrease slightly from the landward sites with concentrations just above 0.5 wt% to the seaward sites with values around 0.3 wt%, although there is considerable variation within all the profiles. While there are relatively small differences in TOC between the landward and seaward locations, methane concentrations show a distinct increase from seaward to landward sites. All landward sites have methane concentrations higher than 10,000 ppmv, with averages around 20,000 ppmv. Several of the sites in the Kumano Forearc Basin and in the accretionary prism have concentrations above 40,000 ppmv, (e.g., C0001, C0002, C0004, and C0008). In contrast, concentrations in both of the seaward sites generally are at or below 1,000 ppmv. The highest values are below 5,000 ppmv at Site C0011 and below 210 ppmv at Site C0012. Low concentrations of higher molecular hydrocarbons, mostly ethane, were observed in all of the cores, typically with values around 10 ppmv. The concentration range for these gases is very similar at landward and seaward sites.

Concentrations of chlorine are generally stable and close to the seawater level of 559 mM. Generally, the values gently decrease downward at Sites C0002, C0006, and C0011, and increase at Sites C0004, C0012, and C0018. The scatter observed in some sites probably is related to the presence of gas hydrates, as fresh water input from gas hydrate dissociation during core recovery is common in cores in accretionary prisms (Hesse, 2003). Gas hydrates were found between 120 and 200 m CSF at Site C0002 and between 70 and 170 m CSF at Site C0008. While the downward patterns of bromine are similar to those of chlorine, they generally show enrichments of 20 to 30% relative to seawater values, reaching ~1200 mM at Sites C0001, C0002, C0004, C0008, and C0018 and ~1000 mM at Sites C0006, C0007, C0011, and C0012.

5.2. Iodine and ^{129}I/I results

Iodine concentration profiles were produced for all nine cores of the NanTroSeize transect, and ^{129}I/I were measured in a subset of the samples from seven cores. Results reported previously (concentrations from Sites C0001, C0002, C0004, and C0008, ratios from C0001 and C0002; Tomaru and Fehn, 2012) are integrated here for the examination of iodine systematics across the study area. In all the landward sites except for the two sites at the prism toe (C0006 and C0007), iodine concentrations increase strongly with depth from the seawater value (0.44 μM) to values around 200 μM beyond 200 m CSF. Values up to 450 μM, corresponding to enrichment factors of 1,000 compared to seawater were observed at Site C0002, which also has the most prominent presence of gas hydrates of all the sites. The increase of iodine concentrations with depth is more modest in the profiles at the two toe sites, which level out at values around 100 μM. In contrast, the profiles for the two sites seaward of the

trough (C0011 and C0012) show hardly any increase with depth and have concentrations close to seawater values.

All the $^{129}I/I$ ratios were found to be at or below the initial seawater ratio (1500×10^{-15}), the starting point at the seawater-sediment interface. Sample volumes were not sufficient to determine ratios in samples close to the seafloor, but it can be assumed that the profiles start at that value. All the profiles decrease with depth, with the most consistent downward decrease in $^{129}I/I$ ratios observed at Site C0001, from 939×10^{-15} at 41 m CSF to $\sim400\times10^{-15}$ at ~200 m CSF, where the lithologic boundary between the old accretionary prism and overlying younger forearc basin sediment is located (red line in Fig. 2). Although the data coverage for Site C0002 is quite limited, it suggests constant values of $\sim400\times10^{-15}$ beyond the lithologic boundary at 922 m CSF (blue line in Fig. 2). The lowest ratios (oldest iodine ages) are observed in some of the sites in the accretionary prism (C0004 and C0008) above the megasplay fault, with a gentle increase in the ratio toward the fault. A very different behavior is apparent at Site C0011, the seaward site located in the Shikoku Basin. Because of the low iodine concentrations there, only two samples provided sufficient material to make AMS determinations, but both of those ratios are close to the pre-anthropogenic value and considerably higher than any of the other ratios measured in the landward cores.

6. DISCUSSION

6.1. Interpretation of iodine concentrations

6.1.1. Iodine and organic material

Concentrations of iodine display the strongest variation of all the halogens at the sites. At all the sites landward of the trough, they strongly exceed the seawater value

of 0.44 μM, except at very shallow levels just below the seafloor, in contrast to the seaward sites, where iodine concentrations are relatively close to seawater values (Fig. 2). Concentrations in pore waters on continental margins are, however, often affected by hydration reactions due to the alteration of volcanic ash or dilution related to clay mineral dehydration at depth (Brumsack et al., 1992; Kastner et al., 1993). Because chlorine is a physicochemically stable halogen in marine environments, its concentration profiles provide a good measure for input or uptake of H_2O and I/Cl profiles describe iodine enrichment more properly without H_2O gain or loss (Fig. 3). Although the behavior of bromine in marine pore water has not been studied well, the amount of organic material influences bromine concentrations (Price et al., 1970; Price and Calvert, 1977) and depth profiles of bromine fall somewhere between those of chlorine and iodine (Fig. 2). The I/Cl profiles as well as I/Br show significant enrichment of iodine with increasing depth in the landward sites, but only slight increases in concentrations in the seaward sites (Fig. 3).

The presence of iodine in marine sediments typically shows a close association with the amount of carbon present in the sediments and iodine concentrations in pore waters often follow the TOC profiles (e.g., Kennedy and Elderfield, 1987). This correlation is obvious at the seaward sites, where TOC values around 0.5 wt% are associated with almost constant values of iodine concentrations, which are only slightly above seawater values. This downward pattern of iodine reflects release of iodine from marine organic materials into pore water with no or minor upward diffusion/advection. Thickness of organic rich sediments within the diagenesis interval is also reflected in the total amount of iodine in pore water, resulting in the variation of iodine enrichment (You et al., 1993; Muramatsu et al, 2007). Sediments within the thermogenic zone,

>50 °C peaking at ~150 °C (Rightmire, 1984), are relatively thin at the seaward sites. The extrapolated temperatures at the bottom of the Shikoku Basin are 62 °C at Site C0011 (1050 m CSF) and 75 °C at Site C0012 (538 m CSF), respectively (Henry et al., 2012). These observations suggest low rates of decomposition, in good agreement with the relatively low concentrations of methane observed in the seaward locations. The modest and linear increases of methane to 5,000 ppmv and iodine to 100 μM at Site C0011 and somewhat less at Site C0012 together with nearly constant TOC around 0.3 wt% possibly reflect continuous release of iodine from low TOC hemipelagic sediments.

The situation is very different at the sites landward of the trough: Rapid increases of iodine concentration are visible in the upper 100 to 200 m CSF and relatively constant values in the deeper section in all the landward sites (Fig. 2). Concentrations reach the highest values in the Kumano Basin (> 400 μM in Site C0002), and somewhat lower values (~100 μM) in the prism toe sites, which are, however, still higher than seawater values by several orders of magnitude. The strong enrichment in iodine in the landward sites is not accompanied by higher concentrations of TOC, in fact the range and variation of TOC observed at all the sites is quite similar around 0.5 wt% (Kinoshita et al., 2009; Saito et al., 2010). Because concentrations of organic material and the age range of sediments are almost identical at landward and seaward sites, the high concentrations of iodine at the landward sites are unlikely to be derived from the decomposition of organic material in the host sediments. A much more likely scenario is that iodine was transported into the current location via advection of aqueous fluids. Similar arguments can be made for the distribution of methane in the cores: Concentrations in the seaward sites are much lower than in all the landward sites, even

though the concentrations of organic material are similar throughout all the sites. It is therefore likely that methane in the landward sites also originated in formations other than the current host sediments.

A distinct change in iodine concentration is observed at Site C0002, from more than 400 μM at 200 m CSF to 200 μM at 480 m CSF, which is more comparable to the other prism sites. Because material was not recovered between 200 and 477 m CSF at Site C0002, the exact location of the transition in the core cannot be identified, but the significant increase probably reflects lateral input of iodine-rich fluids that are also enriched in methane. Fluid of that type has been suggested to be responsible for the accumulation of gas hydrates in sandy layers in this interval (Muramatsu et al., 2007; Tomaru et al., 2007a; Miyakawa et al., 2014).

6.1.2. Iodine and methane

The enrichment in iodine in the cores is accompanied by a similar behavior of methane, an observation common to many other locations with gas hydrates or other methane rich fluids (e.g., Martin et al., 1993; Egeberg and Dickens, 1999; Lu et al., 2011). The transect allows a close look at the behavior of methane and other hydrocarbon gases in locations on both sides of the trench. All the landward sites reach methane concentrations which are higher by one or more orders of magnitude than those at the seaward sides. Because sediment ages are similar for all the cores and presence of organic material differs only slightly between seaward and landward sites, methane in the landward sites probably has sources outside the host sediments. The similarity in transport behavior between iodide and methane in aqueous fluids (Boudreau, 1997) suggests that these two compounds were transported into their present locations from

the same source, i.e. deeper layers in the upper plate.

Together with methane/ethane (C_1/C_2) ratios, $\delta^{13}C$ values in methane were determined at all the landward sites, and the results point to a strong dominance of biogenic gases in these sites (Toki et al., 2012). Heat flow values in the accretionary prism range between 27 and 52 °C/km (Henry et al., 2012), i.e. they are too low to provide temperatures sufficient for the production of thermogenic methane in these cores. The C_1/C_2 ratios at the two seaward (Sites C0011 and C0012) sites are below 400, which usually are interpreted as sign of thermogenic production of hydrocarbons (Saito et al., 2010; Henry et al., 2012). However, low amounts of higher hydrocarbons, such as observed in these cores, can also be produced by biological processes in marine sediments (Hinrichs et al., 2006), so that the low C_1/C_2 ratio is not necessarily indicative of thermogenic production of these gases here. The measured heat flow values in these cores (56 °C/km at C0011 and 135 °C/km at C0012, Henry et al., 2012) also make it unlikely that temperatures for thermogenic production were reached in these sites.

6.2. Interpretation of iodine ages

6.2.1. $^{129}I/I$ ratio and iodine age

The main observations related to the iodine distribution in the NanTroSEIZE transect are the strong increase in concentrations with depth at the landward sites, and the decrease in concentrations from landward to seaward sites. Changes in the concentration of organic materials as well as methane are relatively small compared to the magnitude of the changes in the observed iodine profiles. It is therefore likely that the concentration profiles reflect addition of iodine from sources outside the host

sediments of the pore waters, a problem that can be addressed with the iodine isotopic system.

The presence of the radioisotope, ^{129}I, provides the opportunity to identify potential source formations for the iodine at the sites, which then allows the construction of transport models for the fluids in this region. The $^{129}I/I$ ratios provide minimum iodine ages based on equation (1) as shown by the upper axis of $^{129}I/I$ ratios in Figure 2, which vary from ages close to 50 Ma in some of the prism sites to less than 6 Ma in the input sediments. The ^{129}I results for the deep section of the accretionary prism, older than 25 Ma, agree well with previous investigations from gas hydrate exploration wells, located ~100 km NE of the present sites (Tomaru et al., 2007a). Figure 4 compares ages of the host sediments (Kinoshita et al., 2009; Saito et al., 2010; Hayashi et al., 2011; Henry et al., 2012; Su, 2012) to the iodine ages of pore waters determined from $^{129}I/I$ ratios. The host sediments cover similar age ranges throughout the transect, but only the iodine ages for the samples from the seaward side are close to those of the host sediments (indicated by the dashed line), while iodine ages for all the samples from the landward side of the trough are clearly older than those of their host sediments. This comparison demonstrates that different sources are responsible for the iodine in landward and seaward sites. Whereas iodine at the seaward sites is derived from material within the host sediments, iodine at the landward sites predominantly must have been transported in from formations with ages older than 25 Ma.

6.2.2. Source formations for iodine

The large discrepancy between ages of host sediments and iodine ages in the pore waters in all the cores landward of the trough indicates that iodine is not derived

locally but transported into the present locations in aquatic fluids. Because the sediments on the incoming plate are younger than 21 Ma, in good agreement with the iodine ages observed at Site C0011, and have relatively low concentrations of iodine and organic material, subducting marine sediments can be ruled out as source for the iodine enrichment at the landward sites. A more likely source is to be found in the upper plate, where formations of Eocene age or older are present due to the tectonic evolution of that region (Okino et al., 1994). High organic productivity is prevalent at continental margins, which are thus often the location of considerable accumulation of organic material (Lu et al., 2011). In the case of the Nankai Trough region, potential source formations with ages between 30 and 50 Ma, i.e., compatible with the range suggested by the iodine results, are present in the backstop which is composed of formations of Eocene age or older (Nakanishi et al., 2002; Dessa et al.,2004; Waseda and Uchida,2004).

The likely source formations are located at depths of 5 km or more and at lateral distances of 10 km or more from the core sites, suggesting that iodine transport has occurred over distances greater than 10 km. Because transport of iodine over distances of this magnitude must occur in aquatic fluids, these observations indicate that fluid flow in active margins can cover tens of kilometers. Model calculations have suggested that transport of this type is quite possible in active margins (e.g., Saffer and Bekins, 2002). The distance between source formations and cored sites allows an estimate of the fluid velocities necessary in these formations. Assuming a distance of 20 km between the source center and depositional sites and that the subduction scenario became active 20 Ma, a flow velocity of 0.1 cm/yr results. These values are, however, only minimum values, because a straight line flow path and onset of movement at the

time of subduction initiation is assumed. The actual flow path probably is very complicated and could include scenarios such as release of the fluids containing the methane and iodine from the source formation and subsequent residence in other formations for considerable time, before movement into the current location. The observation, that the dominant phase of methane in the fluids is of biogenic origin, indicates that the formation of the methane occurred while the source formations were still at relatively shallow levels, but because the isotopic composition of methane is unlikely to change after it has formed, later exposure to higher temperatures, as for the indicated source formations, would not affect the isotopic composition of the methane.

Regardless of the specific pathways and travel history, the fluids must have covered the distance from the source to the surface estimated above. The driving forces for fluid flow in active margins, such as seismic pumping or other forces related to plate movement are very intermittent in their nature. With these considerations, flow velocities related to subduction processes probably are one or two orders of magnitude greater than estimated here, which would bring them into ranges projected for hydrothermal convection at Mid-Ocean Ridges (e.g., Fehn et al., 1983) or large-scale gravitational flow (e.g., Bentley et al., 1986; Garven, 1995).

The situation is different for the two sites in the seaward Shikoku Basin, characterized by low iodine concentrations, low organic materials and relatively young iodine ages, which are compatible with the ages of the host sediments and possibly seawater. Although the concentration profiles reach all the way to the basaltic basement (Site C0012) or close to it (Site C0011), none of them show indications of fluid flow. This observation supports the result for the two isotope ratios measured at Site C0011, which demonstrate that iodine was derived from the local sediments. Ethane and

propane were observed at these sites, the presence of which can be interpreted as an indicator of advection (Saito et al., 2010). Because low concentrations, as seen here, can also be produced by in-situ biological processes (Hinrichs et al., 2006), the presence of these gases does not necessarily indicate advection in this case. Seismic activity associated with the subduction apparently does not trigger fluid flow on the seaward side of the trough and contributions of old iodine from the landward sites is absent at these hemipelagic sites.

6.3. Influence of structural discontinuities on fluid flow

As an active margin, the Nankai Trough region has many tectonic structures such as the megasplay fault system, the decollement or depositional discontinuities, which could have observable influence on the fluid flow distribution. One example is the drop of sediment porosity observed at ~200 m CSF at Site C0001, from ~60% below the boundary to ~50% above, resulting in an 11% decrease in permeability (Yue et al., 2012). Although these changes are rather small, they might slow the upward migration of fluids carrying old iodine and result in the somewhat younger age observed just above this boundary.

Two of the sites (Sites C0004 and C0008) cross the megasplay fault system, identified in earlier investigations (Seno et al., 1993), which has been suggested as a conduit for fluids (Lauer and Saffer, 2012). A slight increase in iodine age with depth is observed there which might be related to the transport of younger iodine from the root of the megasplay fault system. The megasplay fault branches at a depth of ~8 km and ~55 km landward from the trough axis. Based on the subduction rate of ~4 to 6 cm/yr between the Philippine Sea Plate and Eurasian Plate, the age of the interface sediments

480 at the branching point is as young as 0.9 Ma (Seno et al., 1993; Heki and Miyazaki, 2001; Park et al., 2002; DeMets et al., 2010). The age of iodine liberated at this point is thus considerably younger than that of the accretionary prism and the $^{129}I/I$ ratio could have been increased in response to the addition of younger iodine, generating the observed downward increase in the $^{129}I/I$ profile (Fig. 2).

485 Fluid delivery through the deformed zone associated with the decollement might also be observable at Sites C0006 and C0007 in the frontal thrust area (Fig. 2), where iodine enrichments are found near the brecciated/fractured zone induced by the frontal thrust activity (Screaton et al., 2009). Of all the cores sampled, the profile at Site C0002 shows the strongest increase in iodine concentrations in the first 200 m. The 490 upper section of this core is part of the Kumano Forearc Basin, while the deeper parts in the accretionary prism show lower concentrations. The profile is similar to several profiles obtained in gas hydrate zones at the Hydrate Ridge, which were related to the presence of considerable lateral flow in this region (Lu et al., 2008). Perhaps the sediment body of the Kumano Forearc Basin have a somewhat higher permeability than 495 the deeper parts of the accretionary prism, allowing for lateral movement of fluids, although the source for all the fluids in this site was identical according to the iodine ages. Because data coverage is limited at these sites, these observations are tentative, but suggest that, with sufficient data coverage, the iodine system is useful for the detection of specific flow paths.

500

6.4. Migration and mixing of iodine

The observed iodine concentrations and $^{129}I/I$ ratios point to the presence of two main types of iodine in the pore waters of the Nankai Trough area (Fig. 5). One

type is best represented in the two seaward cores (Sites C0011 and C0012): Iodine concentrations there are mostly below 10 μM, i.e., only slightly higher than seawater values, and show only a modest increase with depth. This iodine originated from organic materials in hemipelagic sediments and was in isotopic equilibrium with seawater at the time of deposition. Because of the low iodine concentrations, $^{129}I/I$ ratios in only two samples could be determined at Site C0011, but both of them were compatible with the ages of their respective host sediments. These results point to the release of iodine from local organic materials with little or no fluid movement within the sediments involved. The slight increase in iodine concentrations with depth probably is caused by the gradual degradation of organic materials with time and the concurrent release of iodine into the pore waters. The concentration profiles for these two cores agree well with others found in deep sea sediments with low concentrations of organic materials (e.g., Martin et al., 1993), but it is the first time that iodine ages verify that local sources are responsible for the iodine in these sediments.

The other major type of iodine is present in all the landward cores. Iodine there is enriched over seawater values by two to three orders of magnitude and has $^{129}I/I$ ratios predominantly below 400×10^{-15}, corresponding to ages of 30 Ma or older. Because the host sediments of samples there are all younger than 7 Ma, iodine could not have been derived locally and must have been transported into their current location by the advection of aqueous fluids. In most landward cores, iodine concentrations gradually increase with depth, with a corresponding decrease in $^{129}I/I$ ratios, best visible in the core at Site C0001. These profiles reflect the mixing between the two types of iodine, especially in the shallow depths of the cores. It is worth noting that sites in other locations with high concentrations of iodine in pore waters are all characterized by the

presence of gas hydrates or other high concentrations of methane (e.g., Lu et al., 2011; Fehn, 2012) as is the case in the landward sites of the Nankai Trough. While mixing between these two sources of iodine are the predominant causes for the shapes of the observed profiles, presence of structural discontinuities might also influence the profiles, such as a change in porosity, fluid flow through the megasplay fault or lateral movement in the shallow layers of the Kumano Forearc Basin.

6.5. Distribution of iodine between fluids and solids in marine sediments

The main goal of this study was the determination of the origin of iodine in the fluids collected from sediments and its relation to flow patterns across an active margin. Iodine concentrations were not directly determined in the sediments themselves, but, because the distribution of iodine in marine sediments is closely tied to that of organic carbon (e.g., Kennedy and Elderfield, 1987), the TOC concentration can be used to estimate the amount of iodine in the solid part of the sediments. An investigation of iodine concentrations in cores from the Peru Margin determined that I/TOC ratios in the solids mostly are close to 1×10^{-4} g/g in situations without gas hydrates present and somewhat higher in locations with gas hydrates (Martin et al., 1993). The similarity in geologic setting between the two active margins allows the use of this value for an estimate of iodine concentrations in the solid phases in the Nankai Trough Transect. At Site C0011, the TOC value varies between 0.1 and 0.4 wt%, which results in iodine concentrations between 0.1 and 0.4 ppm. Using a porosity of 50% (Fig. 2) and a density of 2 g/cm^3, the volumetric concentration of iodine is between 0.1 and 0.4 μg/cm^3 in the solid phase. The concentrations in the fluids vary between 10 and 50 μM (Fig. 2), which, using the same porosity, translates to values between 0.5 and 2.5 μg/cm^3 at Site C0011.

Although these calculations provide only rough estimates, they demonstrate that even at the low concentrations in the seaward sites the majority of iodine is contained in the fluids. Further addition of iodine from the disintegration of organic materials is possible, but would, at most, double the concentrations in these cores and would not affect the isotopic ratio, because iodine in the incoming sediments has similar ages as those observed in the fluids. While organic materials in the local sediments have contributed to the iodine budget in all of the fluids, it is the major source only in the seaward sites, but not in the landward sites.

The high concentrations in the landward fluids suggest that the source formations had considerably higher organic materials present than found in the sediment cores here. All the measured TOC concentrations in this study are below 1 wt%, with most of the values around 0.5 wt%. Because these values are lower by one order of magnitude or more compared to other sites (e.g., Martin et al., 1993), it is not hard to image that the potential source regions had sufficient organic material to supply the observed iodine in the fluids on the landward sites.

6.6. A model for fluid transport in the Nankai Trough area

Figure 6A compares the analytical results across thetransect, with concentrations and ages of the oldest iodine sample at each site and the age of the respective host sediments. The proposed mode of iodine transport across the NanTroSEIZE transect based on the ^{129}I system in pore waters is summarized in Fig. 6B. The ages are relatively constant at >30 Ma throughout the sediment column at the landward site, suggesting that iodine there is derived from similar lithologic units related to the old backstop positioned landward of the core sites. These units probably

contain substantial amounts of organic materials, accumulated over 50 Myrs or more, which is the likely source of the iodine in the pore waters. The migration of the fluids carrying old iodine might be impeded at unconformities such as the lithologic boundary found at Site C0001, or might show the addition of substantial amounts of iodine via lateral movement as at Site C0002. The situation is very different in the Shikoku Basin hemipelagic sediment overlying the subducting Philippine Sea Plate. Iodine concentrations in these locations are only slightly above those in seawater, suggesting that little, if any, iodine is transported within these sediments. Although $^{129}I/I$ ratios in only two samples could be measured in these cores, the results are compatible with this interpretation, i.e., they are of similar age as the host sediments and do not show migration into the current locations. As marine sediments travel past the trough into the subduction zone, relatively young iodine might be mobilized and added to the fluids traveling through the megasplay fault zone and the decollement. These additions could explain the younger ages observed in the fluids close to these structural discontinuities.

Although the results derived from the ^{129}I system are directly applicable only to questions concerning origin and migration of iodine, they provide insights for the movement of fluids and other compounds in this area. Transport of iodine over the distances postulated here must have occurred in aqueous fluids, which, although not necessarily as old as the iodine, must have reached the deep source formations or originated there to bring iodine to the current locations. Cores with high iodine concentrations were all found on the landward side of the trough system, typically associated with high concentrations of methane. The change from low methane concentrations in the seaward sites to very high concentrations in the landward sites follows closely that of the iodine concentrations. Just like iodine, methane is also

derived from organic material and has very similar transport characteristics in aqueous fluids (Boudreau, 1997), which has resulted in a close correlation between the occurrence of methane and the enrichment of iodine in marine fluids (e.g., Martin et al., 1993; Egeberg and Dickens, 1999, Lu et al., 2011).

7. CONCLUSIONS

The iodine isotope system together with halogen systematics was applied for the understanding of sources and migration paths for iodine-carrying fluids in the accretionary system along the NanTroSEIZE transect. It is the first investigation, in which the iodine system was used to compare sites on both sides of an active subduction zone. Samples came from nine cores covering sites in sediments of the Shikoku Basin at the seaward side of the trough as well as in the accretionary prism and the Kumano Forearc Basin at the landward side. In all landward cores, iodine concentrations are strongly enriched compared to seawater values, reaching values above 400 μM, but are close to seawater values in the seaward sites. The differences are also visible in iodine ages: At all landward sites ages reach values between 30 and 50 Ma, i.e., considerably older than those in the host sediments, but ages are very close to those of the host sediments at the seaward sites.

The low iodine concentrations observed at the seaward sites probably are related to the release of iodine from organic matter and, because iodine ages at the seaward sites are compatible with those of the host sediments, only local transport of iodine occurs there. This compatibility between iodine ages and sediment ages at the seaward sites also is in excellent agreement with the interpretation of earlier ^{129}I results, related to the transport of marine sediments into subduction zones and subsequent

release of volatiles from subduction volcanoes (e.g., Snyder and Fehn, 2002; Fehn, 2012).

In contrast, the $^{129}I/I$ data at the landward sites as well as the high iodine concentrations demonstrate that iodine in pore waters there was transported from old accreted sediments in the forearc area. The potential source areas are at distances of more than 10 km from the sample sites, indicating that large scale fluid movement occurs in the upper plate. The distribution of iodine ages in these sites might also reflect the influence of structural features, such as the megasplay fault or the decollement, on the transport of fluids in this region. The similarities observed in the systematics of iodine and methane concentrations in this transect together with their matches in transport characteristics indicate that iodine and methane are derived from the same sources in the upper plate and carried by aquatic fluids over distances in excess of 10 km into the current locations at the landward sites of the trough.

REFERENCES

Bentley, H. W., Phillips, F. M., Davis, S. N., Habermehl, M. A., Airey, P. L., Calf, G. E., Elmore, D., Gove, H. E. and Torgersen, T. (1986) Chlorine 36 dating of very old groundwater: 1. The Great Artesian Basin, Australia. Water Resources Research 22, 1991-2001.

Boudreau, B. P. (1997) Diagenetic Models and Their Implementation: Modelling Transport and Reactions in Aquatic Sediments. Springer, Berlin/New York.

Broecker, W. S. and Peng, T. H. (1982) Tracers in the Sea. Eldigio Press, Palisades, NY.

Brumsack, H. -J., Zuleger, E., Gohn, E. and Murray, R. W. (1992) Stable and radiogenic isotopes in pore waters from Leg 127, Japan Sea, in: Pisciotto, K. A., Ingle, J. C. J., von Breymann, M. T., Barron, J., et al. (Eds.), Proceedings of the Ocean Drilling Program, Scientific Results. Ocean Drilling Program, pp. 635-650.

Burton, J. D. (1996) The ocean: a global geochemical system, in: Summerhayes, C. P., Thorpe, S. A. (Eds.), Oceanography: an illustrated guide. Manson, London, pp. 165-181.

Conin, M., Henry, P., Godard, V. and Bourlange, S. (2012) Splay fault slip in a subduction margin, a new model of evolution. Earth and Planetary Science Letters 341-344, 170-175.

DeMets, C., Gordon, R. G. and Argus, D. F. (2010) Geologically current plate motions. Geophysical Journal International 181, 1-80.

Dessa, J. X., Operto, S., Kodaira, S., Nakanishi, A., Pascal, G., Virieux, J. and Kaneda, Y. (2004) Multiscale seismic imaging of the eastern Nankai trough by full waveform inversion. Geophysical Research Letters 31, 18606, doi:10.1029/2004GL020453.

Egeberg, P. K. and Dickens, G. R. (1999) Thermodynamic and pore water halogen constraints on gas hydrate distribution at ODP Site 997 (Blake Ridge). Chemical Geology 153, 53-79.

Elderfield, H. and Truesdale, V. W. (1980) On the biophilic nature of iodine in seawater. Earth and Planetary Science Letters 50, 105-114.

Fehn, U. (2012) Tracing Crustal Fluids: Applications of Natural ^{129}I and ^{36}Cl. Annual Review of Earth and Planetary Sciences 40, 45-67.

Fehn, U., Green, K. E., Von Herzen, R. P. and Cathles, L. M. (1983) Numerical models for the hydrothermal field at the Galapagos Spreading Center. Journal of Geophysical Research: Solid Earth 88, 1033-1048.

Fehn, U., Holdren, G. R., Elmore, D., Brunelle, T., Teng, R. and Kubik, P. W. (1986) Determination of natural and anthropogenic ^{129}I in marine sediments. Geophysical Research Letters 13, 137-139.

Fehn, U., Peters, E. K., Tullai-Fitzpatrick, S., Kubik, P. W., Sharma, P., Teng, R. T. D., Gove, H.E. and Elmore, D. (1992) ^{129}I and ^{36}Cl concentrations in waters of the eastern Clear Lake Area, California: Residence times and source ages of hydrothermal fluids. Geochimica et Cosmochimica Acta 56, 2069-2079.

Fehn, U., Snyder, G. T. and Egeberg, P. K. (2000) Dating of pore waters using ^{129}I: Relevance for the origin of marine gas hydrates. Science 289, 2332-2335.

Fehn, U., Snyder, G. T., Matsumoto, R., Muramatsu, Y. and Tomaru, H. (2003) Iodine dating of pore waters associated with gas hydrates in the Nankai area, Japan. Geology 31, 521-524.

Fehn, U., Lu, Z. and Tomaru, H. (2006) Data report: $^{129}I/I$ ratios and halogen concentrations in pore water of Hydrate Ridge and their relevance for the origin of

gas hydrates: a progress report, in: Trehu, A.M., Bohrmann, G., Torres, M.E., Colwell, F.S. (Eds.), Proceedings of the Ocean Drilling Program, Scientific Results, College Station, TX, pp. 1-25.

Fehn, U., Snyder, G. T. and Muramatsu, Y. (2007a) Iodine as a tracer of organic material: ^{129}I results from gas hydrate systems and fore arc fluids. Journal of Geochemical Exploration 95, 66-80.

Fehn, U., Moran, J. E., Snyder, G. T. and Muramatsu, Y. (2007b) The initial ^{129}I/I ratio and the presence of 'old' iodine in continental margins. Nuclear Instruments and Methods in Physics Research B 259, 496-502.

Fuge, R. and Johnson, C.C. (1986) The geochemistry of iodine - a review. Environmental Geochemistry and Health 8, 31-54.

Garven, G. (1995) Continental-scale groundwater flow and geologic processes. Annual Review of Earth And Planetary Sciences 23, 89-118.

Harvey, G.R. (1980) A study of the chemistry of iodine and bromine in marine sediments. Marine Chemistry 8, 327-332.

Hayashi, H., Asano, S., Yamashita, Y., Tanaka, T. and Nishi, H. (2011) Data report: late Neogene planktonic foraminiferal biostratigraphy of the Nankai Trough, IODP Expedition 315, in: Kinoshita, M., Tobin, H., Ashi, J., Kimura, G., Lallemant, S., Screaton, E.J., Curewitz, D., Masago, H., Moe, K.T., the Expedition 314/315/316 Scientists (Eds.), Proceedings of the Integrated Ocean Drilling Program. Integrated Ocean Drilling Program Management International, Inc., Washington, DC.

Heki, K. and Miyazaki, S. (2001) Plate convergence and long-term crustal deformation. Geophysical Research Letters 28, 2313-2316.

Henry, P., Kanamatsu, T., Moe, K. and the Expedition 333 Scientists (2012) Proceedings of the Integrated Ocean Drilling Program. Integrated Ocean Drilling Program Management International, Inc., Washington, DC.

Hesse, R. (2003) Pore water anomalies of submarine gas-hydrate zones as tool to assess hydrate abundance and distribution in the subsurface. What have we learned in the past decade? Earth-Science Reviews 61, 149-179.

Hinrichs, K. U., Hayes, J. M., Bach, W., Spivack, A. J., Hmelo, L. R., Holm, N. G., Johnson, C. G. and Sylva, S. P. (2006) Biological formation of ethane and propane in the deep marine subsurface. Proceedings of the National Academy of Sciences of the United States of America 103, 14684-14689.

Jarrard, R. D. (1986) Relations among subduction parameters. Reviews of Geophysics 24, 217-284.

Kastner, M., Elderfield, H., Jenkins, W. J., Gieskes, J. M. and Gamo, T. (1993) Geochemical and Isotopic Evidence for Fluid Flow in the Western Nankai Subduction Zone, Japan, in: Hill, I.A., Taira, A., Firth, J. V. (Eds.), Proceedings of the Ocean Drilling Program, Scientific Results. Ocean Drilling Program, College Station, TX, pp. 397-413.

Kennedy, H. A. and Elderfield, H. (1987) Iodine Diagenesis in Pelagic Deep-Sea Sediments. Geochimica et Cosmochimica Acta 51, 2489-2504.

Kinoshita, M., Tobin, H., Ashi, J., Kimura, G., Lallemant, S., Screaton, E. J., Curewitz, D., Masago, H., Moe, K. T. and the Expedition 314/315/316 Scientists (2009) Proceedings of the Integrated Ocean Drilling Program. Integrated Ocean Drilling Program Management International, Inc., Washington, DC.

Kobayashi, K., Kasuga, S. and Okino, K. (1995) Shikoku Basin and its margins, in:

Taylor, B. (Ed.), Backarc Basins: Tectonics and Magmatism. Plenum, New York, pp. 381-405.

Kodaira, S., Takahashi, N., Park, J. -O., Mochizuki, K., Shinohara, M. and Kimura, S. (2000) Western Nankai Trough seismogenic zone: Results from a wide-angle ocean bottom seismic survey. Journal of Geophysical Research 105, 5887-5905.

Lauer, R. M. and Saffer, D. M. (2012) Fluid budgets of subduction zone forearcs: The contribution of splay faults. Geophysical Research Letters 39.

Lu, Z., Fehn, U., Tomaru, H., Elmore, D. and Ma, X. (2007) Reliability of ^{129}I/I ratios produced from small sample masses. Nuclear Instruments and Methods in Physics Research B 259, 359-364.

Lu, Z., Tomaru, H. and Fehn, U. (2008) Iodine ages of pore waters at Hydrate Ridge (ODP Leg 204), Cascadia Margin: Implications for sources of methane in gas hydrates. Earth and Planetary Science Letters 267, 654-665.

Lu, Z., Tomaru, H. and Fehn, U. (2011) Comparison of iodine dates from mud volcanoes and gas hydrate occurrences: relevance for the movement of fluids and methane in active margins. American Journal of Science 311, 632-650.

Martin, J. B., Gieskes, J. M., Torres, M. and Kastner, M. (1993) Bromine and iodine in Peru margin sediments and pore fluids: implications for fluid origins. Geochimica et Cosmochimica Acta 57, 4377-4389.

Miyakawa, A., Saito, S., Yamada, Y., Tomaru, H., Kinoshita, M. and Tsuji, T. (2014) Gas hydrate saturation at Site C0002, IODP Expeditions 314 and 315, in the Kumano Basin, Nankai trough. Island Arc 23, 142-156.

Moran, J., Oktay, S., Santschi, P. H. and Schink, D. R. (1999) Atmospheric Dispersal of 129Iodine from Nuclear Fuel Reprocessing Facilities. Environmental Science &

Technology 33, 2536-2542.

Moran, J. E., Fehn, U. and Teng, R. T. D. (1998) Variations in $^{129}I/^{127}I$ ratios in recent marine sediments: evidence for a fossil organic component. Chemical Geology 152, 193-203.

Muramatsu, Y., Doi, T., Tomaru, H., Fehn, U., Takeuchi, R. and Matsumoto, R. (2007) Halogen concentrations in pore waters and sediments of the Nankai Trough, Japan: Implications for the origin of gas hydrates. Applied Geochemistry 22, 534-556.

Muramatsu, Y. and Wedepohl, K.H. (1998) The distribution of iodine in the earth's crust. Chemical Geology 147, 201-216.

Nakanishi, A., Kodaira, S. and Park, J. -O. (2002) Deformable backstop as seaward end of coseismic slip in the Nankai Trough seismogenic zone. Earth and Planetary Science Letters 203, 255-263.

Okino, K., Shimakawa, Y. and Nagaoka, S. (1994) Evolution of the Shikoku Basin. Journal of Geomagnetism and Geoelectricity 46, 463-479.

Park, J. -O., Tsuru, T., Kodaira, S., Cummins, P. R. and Kaneda, Y. (2002) Splay Fault Branching Along the Nankai Subduction Zone. Science 297, 1157-1160.

Plank, T. and Langmuir, C. H. (1998) The chemical composition of subducting sediment and its consequences for the crust and mantle. Chemical Geology 145, 325-394.

Price, N. B. and Calvert, S. E. (1977) The contrasting geochemical behaviors of iodine and bromine in recent sediments from the Namibian shelf. Geochimica et Cosmochimica Acta 41, 1769-1775.

Price, N. B., Calvert, S. E. and Jones, P. G. W. (1970) The distribution of iodine and bromine in the sediments of the South Western Barents Sea. Journal of Marine

Research 28, 22-34.

Rao, U. and Fehn, U. (1999) Sources and reservoirs of anthropogenic iodine-129 in western New York. Geochimica et Cosmochimica Acta 63, 1927-1938.

Rightmire, C. T. (1984) Coalbed methane resource, in: Rightmire, C. T., Eddy, G. E., Kirr, J. N. (Eds.), Coalbed methane resources of the United States. American Association of Petroleum Geologists, pp. 1-13.

Saffer, D. M. and Bekins, B. A. (2002) Hydrologic controls on the morphology and mechanics of accretionary wedges. Geology 30, 271-274.

Saito, S., Underwood, M. B., Kubo, Y. and the Expedition 322 Scientists (2010) Proceedings of the Integrated Ocean Drilling Program. Integrated Ocean Drilling Program Management International, Inc., Washington, DC.

Santschi, P. H. and Schwehr, K. A. (2004) $^{129}I/^{127}I$ as a new environmental tracer or geochronometer for biogeochemical or hydrodynamic processes in the hydrosphere and geosphere: the central role of organo-iodine. Science of the Total Environment 321, 257-271.

Screaton, E., Kimura, G., Curewitz, D., Moore, G. and the Expedition 316 Scientific Party (2009) Interactions between deformation and fluids in the frontal thrust region of the NanTroSEIZE transect offshore the Kii Peninsula, Japan: results from IODP Expedition 316 Sites C0006 and C0007. Geochemistry, Geophysics, Geosystems 10.

Seno, T., Stein, S. and Gripp, A. (1993) A Model for the Motion of the Philippine Sea Plate Consistent With NUVEL‐1 and Geological Data. Journal of Geophysical Research 98, 17941-17948.

Sharma, P., Bourgeois, M., Elmore, D., Granger, D., Lipschutz, M. E., Ma, X., Miller, T.,

Mueller, K., Rickey, F., Simms, P. and Vogt, S. (2000) PRIME lab AMS performance, upgrades and research applications. Nuclear Instruments and Methods in Physics Research B(172), 112-123.

Snyder, G. T. and Fehn, U. (2002) Origin of iodine in volcanic fluids: ^{129}I results from the Central American Volcanic Arc. Geochimica et Cosmochimica Acta, 66, 3827-3838.

Snyder, G. T., Aldahan, A. and Possnert, G. (2010) Global distribution and long-term fate of anthropogenic ^{129}I in marine and surface water reservoirs. Geochemistry, Geophysics, Geosystems 11, Q04010.

Su, X. (2012) Data report: occurrence of age-diagnostic nannofossil and biostratigraphic datums at IODP Expedition 316 Sites C0004 and C0008, Nankai Trough, in: Kinoshita, M., Tobin, H., Ashi, J., Kimura, G., Lallemant, S., Screaton, E. J., Curewitz, D., Masago, H., Moe, K. T., the Expedition 314/315/316 Scientists (Eds.), Proceedings of the Integrated Ocean Drilling Program. Integrated Ocean Drilling Program Management International, Inc., Washington, DC.

Toki, T., Uehara, Y., Kinjo, K., Ijiri, A., Tsunogai, U., Tomaru, H. and Ashi, J. (2012) Methane production and accumulation in the Nankai accretionary prism: Results from IODP Expeditions 315 and 316. Geochemical Journal 46, 89-106.

Tomaru, H., Lu, Z., Fehn, U., Muramatsu, Y. and Matsumoto, R. (2007a) Age variation of pore water iodine in the eastern Nankai Trough, Japan: Evidence for different methane sources in a large gas hydrate field. Geology 35, 1015-1018.

Tomaru, H., Lu, Z., Snyder, G.T., Fehn, U., Hiruta, A. and Matsumoto, R. (2007b) Origin and age of pore waters in an actively venting gas hydrate field near Sado Island, Japan Sea: Interpretation of halogen and ^{129}I distributions. Chemical Geology 236, 350-366.

Tomaru, H. and Fehn, U. (2012) Data report: distribution of iodine concentration and ^{129}I in interstitial fluid in the Nankai Trough accretionary prism collected during IODP Expeditions 315 and 316, in: Kinoshita, M., Tobin, H., Ashi, J., Kimura, G., Lallemant, S., Screaton, E. J., Curewitz, D., Masago, H., Moe, K. T., the Expedition 314/315/316 Scientists (Eds.), Proceedings of the Integrated Ocean Drilling Program. Integrated Ocean Drilling Program Management International, Inc., Washington, DC. doi: 10.2204/iodp.proc.314315316.220.2012

Ullman, W. J. and Aller, R. C. (1980) Dissolved iodine flux from estuarine sediments and implications for the enrichment of iodine at the sediment water interface. Geochimica et Cosmochimica Acta 4, 1177-1184.

Ullman, W. J. and Aller, R. C. (1983) Rates of iodine remineralization in terrigenous near-shore sediments. Geochimica et Cosmochimica Acta 47, 1423-1432.

Waseda, A. and Uchida, T. (2004) The geochemical context of gas hydrate in the eastern Nankai Trough. Resource Geology 54, 69-78.

You, C. -H., Gieskes, J. M., Chen, R. F., Spivack, A. and Gamo, T. (1993) Iodide, Bromide, Manganese, Boron, and Dissolved Organic Carbon in Interstitial Waters of Organic Carbon-Rich Marine Sediments: Observations in the Nankai Accretionary Prism, in: Hill, I. A., Taira, A., Firth, J. V. (Eds.), Proceedings of the Ocean Drilling Program, Scientific Results. Ocean Drilling Program, College Station, TX, pp. 165-174.

Yue, L., Likos, W. J., Guo, J. and Underwood, M. B. (2012) Data report: permeability of mud(stone) samples from Site C0001, IODP Expedition 315, Nankai Trough: NanTroSEIZE Stage 1, in: Kinoshita, M., Tobin, H., Ashi, J., Kimura, G., Lallemant, S., Screaton, E. J., Curewitz, D., Masago, H., Moe, K. T., the

Expedition 314/315/316 Scientists (Eds.), Proceedings of the Integrated Ocean Drilling Program. Integrated Ocean Drilling Program Management International, Inc., Washington, DC.

ACKNOWLEDGEMENTS

This research used samples and data provided by the Integrated Ocean Drilling Program, Expeditions 315, 316, 322, and 333. We thank the crew and technical staff of the D/V *Chikyu* for making this expedition a success. We are grateful for ^{129}I/I determinations at PRIME Lab, Purdue University. We acknowledge the comments by three reviewers, which significantly improved this manuscript. This study was financially supported by Japan Agency for Marine-Earth Science and Technology, National Science Foundation, and Research Fellowships for Young Scientists provided by the Japan Society for the Promotion of Science.

FIGURE CAPTIONS

Fig. 1 (A) Location of research area. (B) Bathymetric map of the Nankai Trough offshore the Japanese main island and locations of Sites C0001 to C00018 cored during IODP Expeditions 315, 316, 322, and 333. Black thick lines indicate the seismic line shown in panel (D). Stars indicate the locations of previous gas hydrate explorations (Fehn et al., 2003; Tomaru et al., 2007a). (C) Detailed bathymetric map of the NanTroSEIZE transect with the seismic line (except Site C0002). (D) Regional seismic image across the cored sites.

Fig. 2 Depth profiles of sediment porosity, total organic carbon (TOC), headspace methane, concentrations of chlorine, bromine, iodine, and ^{129}I/I ratio with iodine age

in pore waters, shown with sediment age. No samples were recovered between 201 and 477 m CSF at Site C0002. Red and blue lines indicate the depths of lithologic boundaries between the overlying Kumano Forearc Basin sediment and underlying accreted sediment at Sites C0001 and C0002, respectively (Kinoshita et al., 2009). Green lines indicate brecciated/fractured zone associated with the megasplay fault (Kinoshita et al., 2009). Black and gray lines indicate brecciated/fractured zone of the main frontal thrust zone (Kinoshita et al., 2009). Light blue and orange lines indicate the lithologic boundary between the Shikoku Basin sediment and underlying igneous basement (Saito et al., 2010). Dashed lines represent seawater values (Burton, 1996; Fehn et al., 2007b).

Fig. 3 Depth profiles of I/Cl and I/Br ratios characterizing iodine enrichment and iodine (bromine) source material. Lines indicate the lithologic boundaries or brecciated/fractured zones as shown in Figure. 2

Fig. 4. Comparison between the ages of host sediments and iodine ages derived from ^{129}I in pore water. The dashed line indicates a ratio of 1:1 between the ages of the host sediment and dissolved iodine. The ages of host sediment including error margins were determined using biostratigraphic ages in Kinoshita et al. (2009), Saito et al. (2010), Henry et al. (2012), Hayashi et al. (2011), and Su (2012).

Fig. 5. 1/I vs. $^{129}I/I$ diagram showing sources and mixing paths of iodine.

Fig. 6. (A) Summary of concentration of iodine dissolved in pore water (open symbol), age of iodine radioisotope (closed symbol) and its host sediment (bar). Samples with oldest iodine at each site are represented. (B) Schematic of iodine migration paths across the NanTroSEIZE transect. Blue colored areas highlight potential sources for old iodine relative to the host sediments: old accreted sediments in the backstop and at the

root of the megasplay fault.

Table 1. Analytical results of $^{129}I/I$ ratio of pore waters from IODP Expeditions 315, 316, 322, and 333.

Site/Hole	Average depth (m CSF)*	Average I (μM)*	$^{129}I/I$ (10^{-15})†	Age (Ma)
C0001E	41.0	71.91	938±98.1	10.6
C0001E	89.6	143.2	825±243	13.6
C0001F	154.3	190.8	545±110	22.9
C0001F	183.9	203.1	817±92.7	13.8
C0001F	226.2	209.2	344±66.9	33.3
C0001F	278.9	196.7	420±40.3	28.9
C0001F	336.1	202.4	388±124	30.6
C0001F	423.0	195.6	383±26.0	31.0
C0002B	741.3	197.3	426±105	28.5
C0002B	984.2	180.8	421±86.3	28.8
C0002D	36.3	187.4	379±16.4	31.2
C0002D	111.9	400.1	246±16.1	41.0
C0004D	246.2	193.1	315±113	35.4
C0004D	345.0	205.7	582±243	21.4
C0006E	130.9	138.9	355±127	32.6
C0006E	312.4	135.6	311±80.1	35.6
C0007ABC	10.3	n.d.	244±23.8	41.1
C0007D	250.4	106.8	289±38.5	37.3
C0007D	383.0	84.36	221±24.7	43.3
C0008AC	20.4	95.01	194±43.6	46.3
C0008A	61.3	168.8	191±18.8	46.7
C0008A	138.0	195.6	237±33.1	41.8
C0008A	211.5	189.0	229±20.7	42.6
C0008C	54.5	169.8	207±49.6	44.9
C0008C	97.5	181.4	246±21.4	40.9
C0008C	163.4	173.2	336±29.0	33.9
C0011D	203.7	27.23	(150±30.0)x10	0.00
C0011D	322.5	32.62	(115±21.0)x10	6.02

*Weighted average depth and concentration were calculated from I concentration and volume of sample aliquots combined in the sample

for $^{129}I/I$ measurement.

†Iodine age is calculated from standard decay equation of ^{129}I with an initial $^{129}I/I$ ratio of 1500×10^{-15}.

n.d.: not determined.

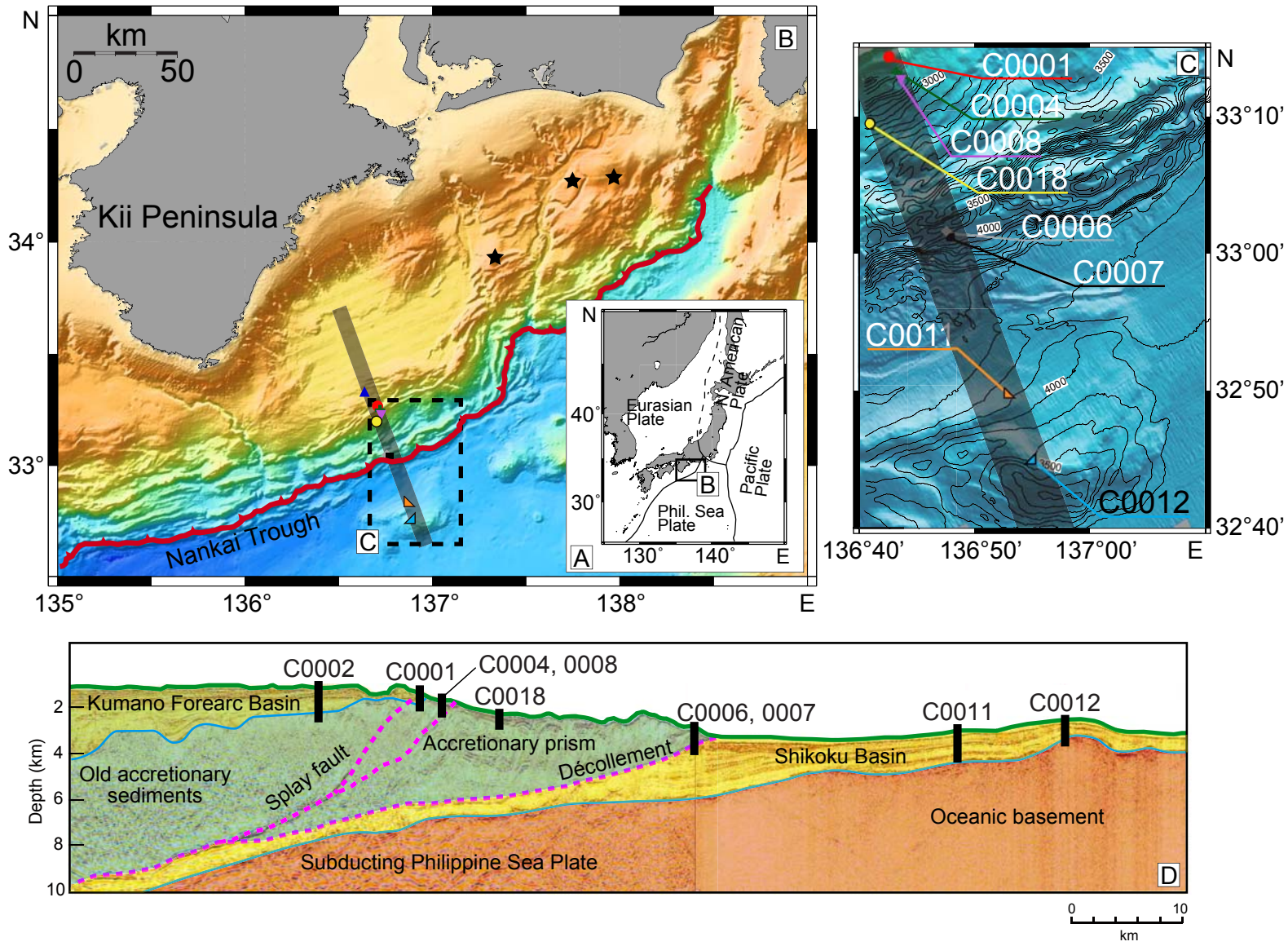
N
km
0
50
B
Kii Peninsula
34°
33°
Nankai Trough
C
135°
136°
137°
138°
E
N
40°
30°
Eurasian Plate
N American Plate
Pacific Plate
Phil. Sea Plate
B
A
130°
140°
E
C0001
C0004
C0008
C0018
C0006
C0007
C0011
C0012
3000
3500
4000
3500
4000
3500
C
N
33°10'
33°00'
32°50'
32°40'
136°40'
136°50'
137°00'
E
C0002
C0001
C0004, 0008
C0018
C0006, 0007
C0011
C0012
Kumano Forearc Basin
Old accretionary sediments
Splay fault
Accretionary prism
Décollement
Shikoku Basin
Oceanic basement
Subducting Philippine Sea Plate
Depth (km)
2
4
6
8
10
D
0
10
km

Fig.1

Fig.2A

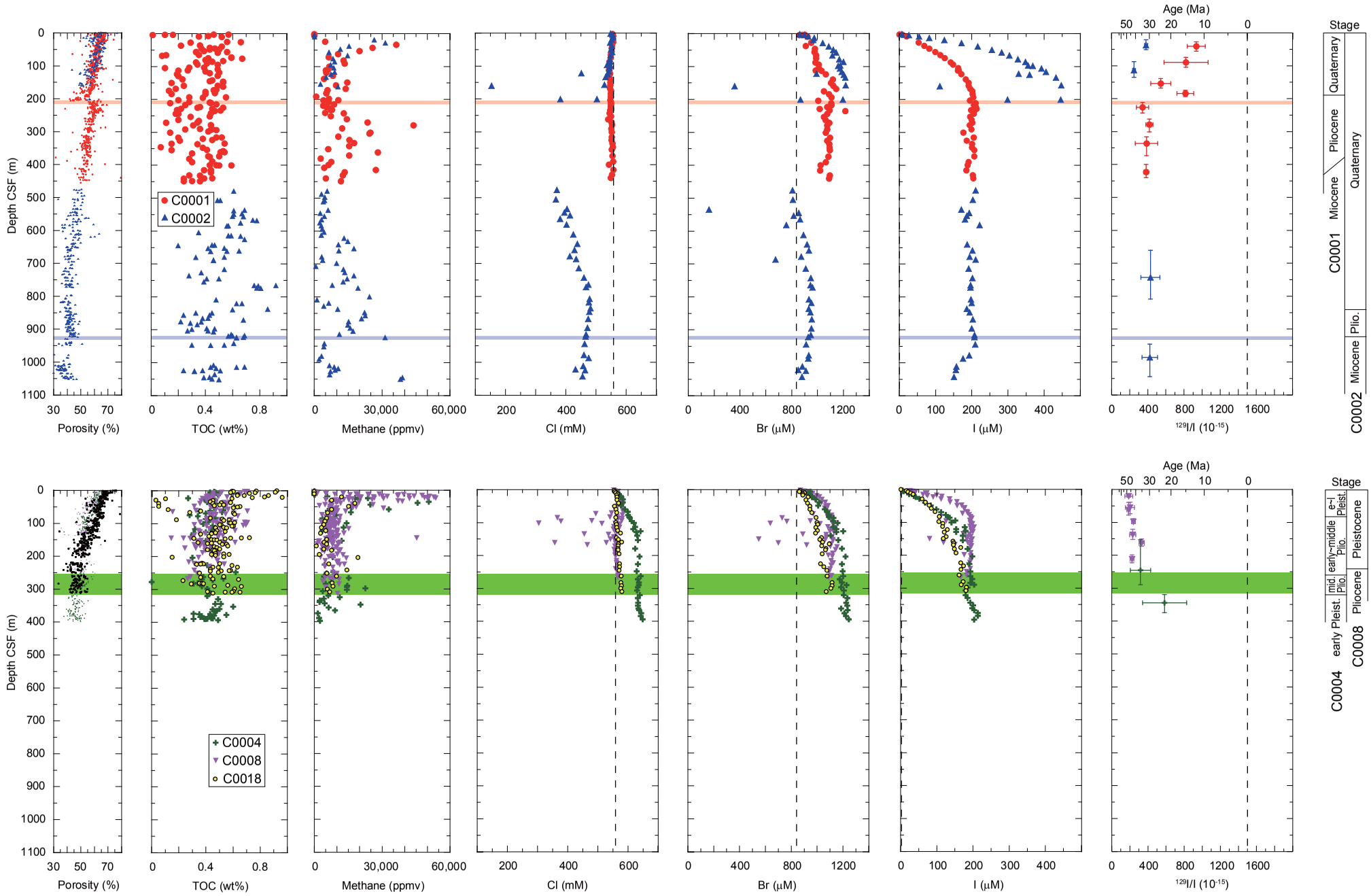
Depth CSF (m)
Porosity (%)
TOC (wt%)
Methane (ppmv)
Cl (mM)
Br (μM)
I (μM)
Age (Ma)
129I/I (10-15)
Stage
C0001
C0002
Quaternary
Pliocene
Miocene
Plio.
C0004
C0008
C0018
early Pleist.
mid. Plio.
early–middle Plio.
e–l Pleist.
Pleistocene

Fig.2B

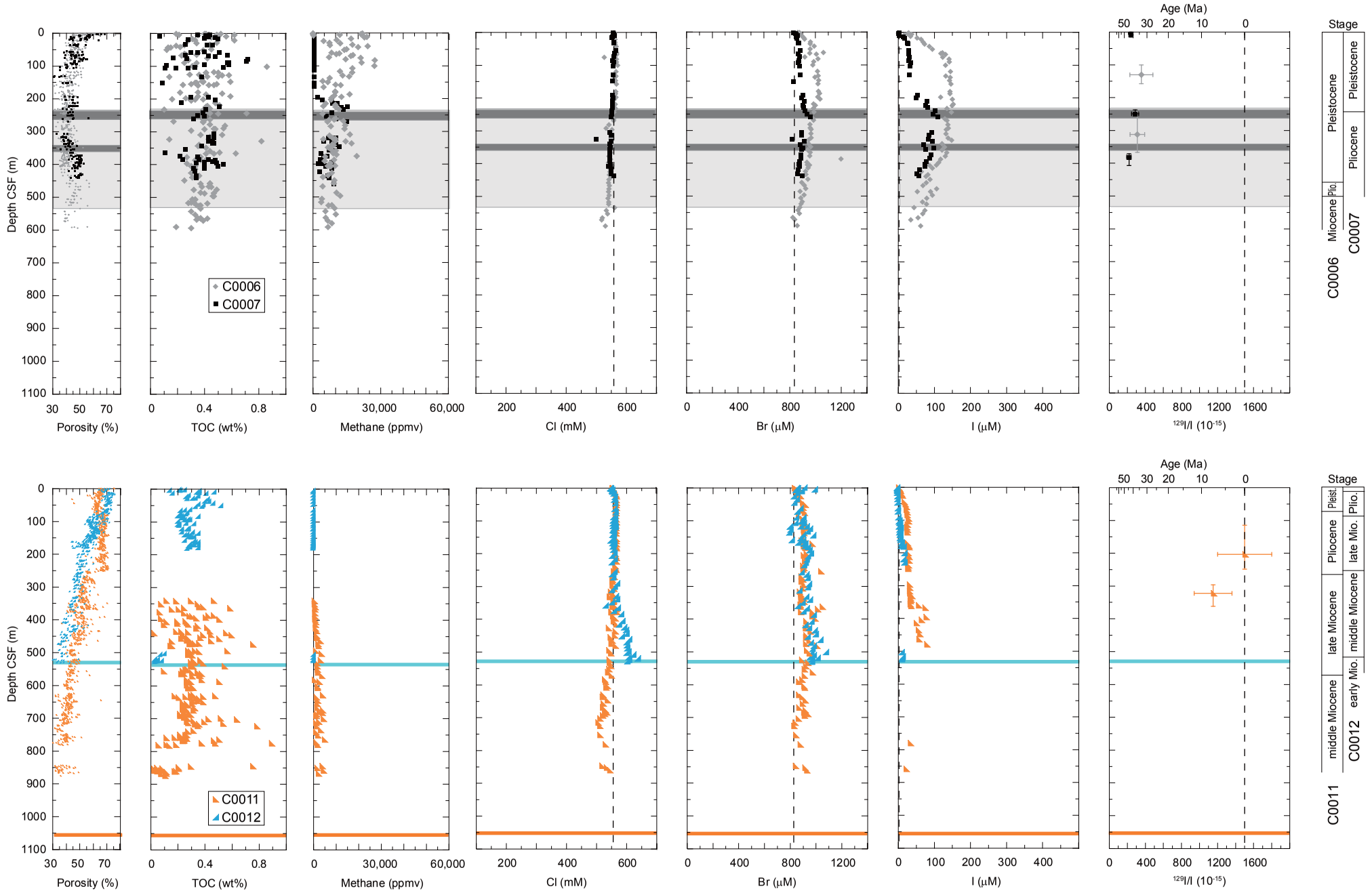
Depth CSF (m)
Porosity (%)
TOC (wt%)
Methane (ppmv)
Cl (mM)
Br (μM)
I (μM)
129I/I (10-15)
Age (Ma)
Stage
C0006
C0007
C0011
C0012
Pleistocene
Pliocene
Miocene
late Miocene
middle Miocene
early Mio.

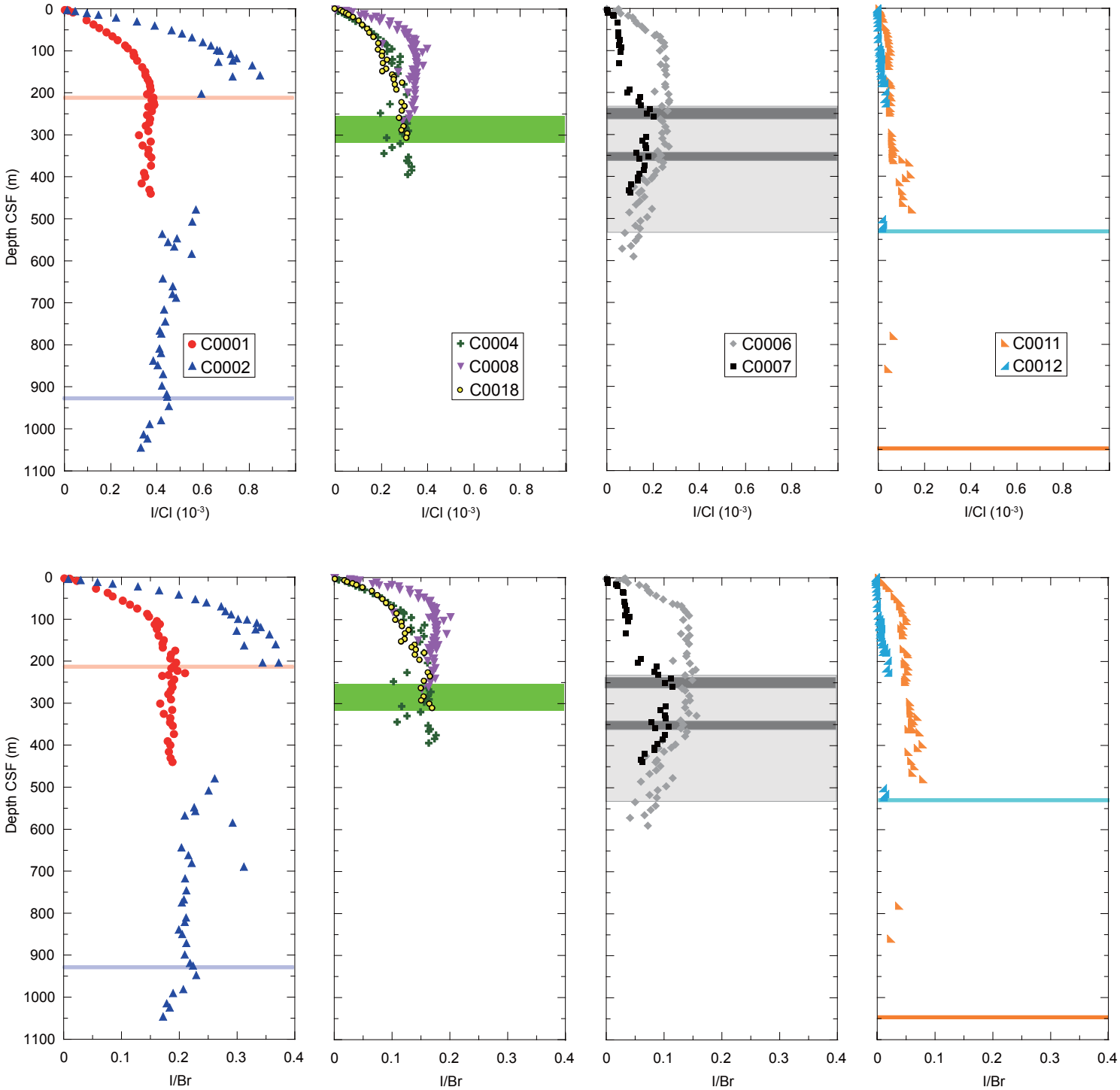
Depth CSF (m)
0
100
200
300
400
500
600
700
800
900
1000
1100
C0001
C0002
C0004
C0008
C0018
C0006
C0007
C0011
C0012
0
0.2
0.4
0.6
0.8
I/Cl (10-3)
0.1
0.3
I/Br

Fig.3

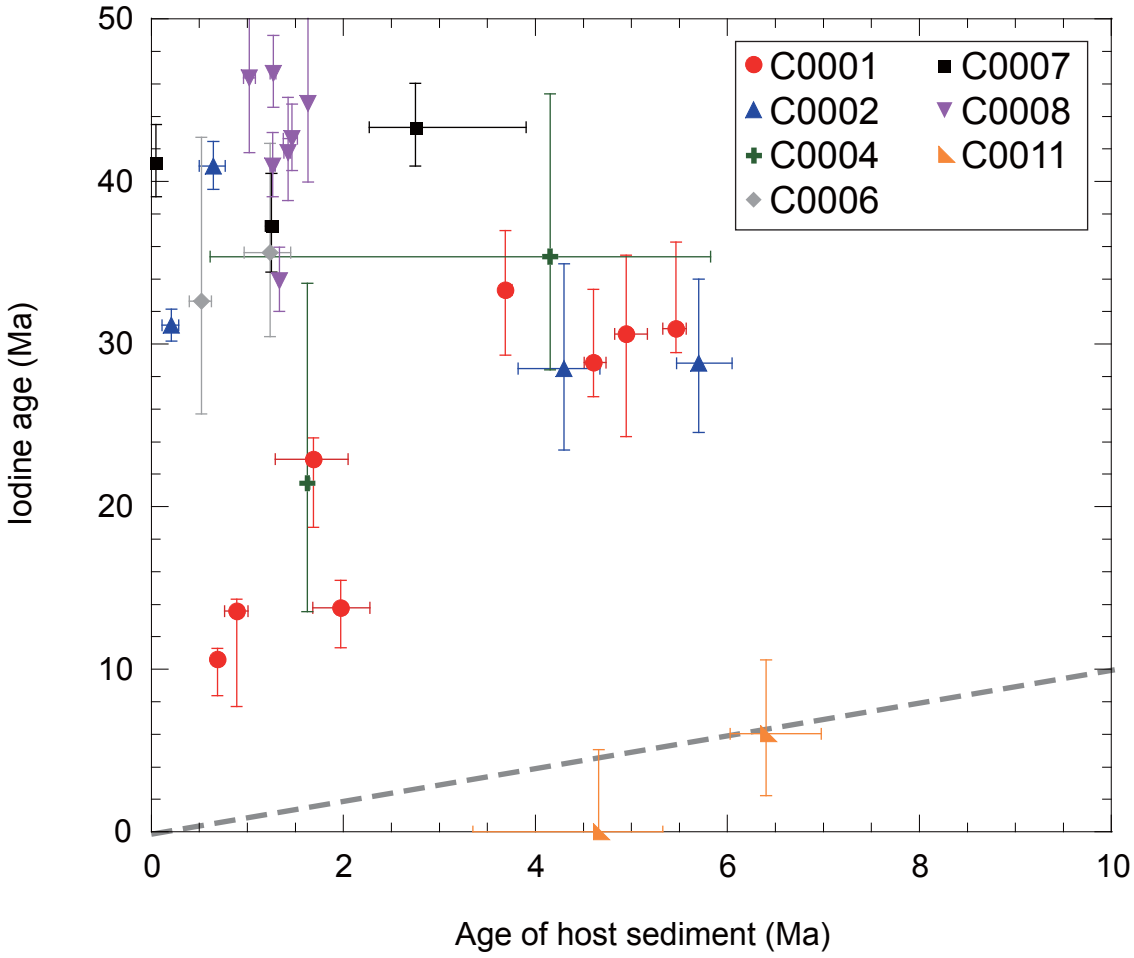
C0001
C0002
C0004
C0006
C0007
C0008
C0011
Iodine age (Ma)
Age of host sediment (Ma)
0
10
20
30
40
50
0
2
4
6
8
10

Fig.4

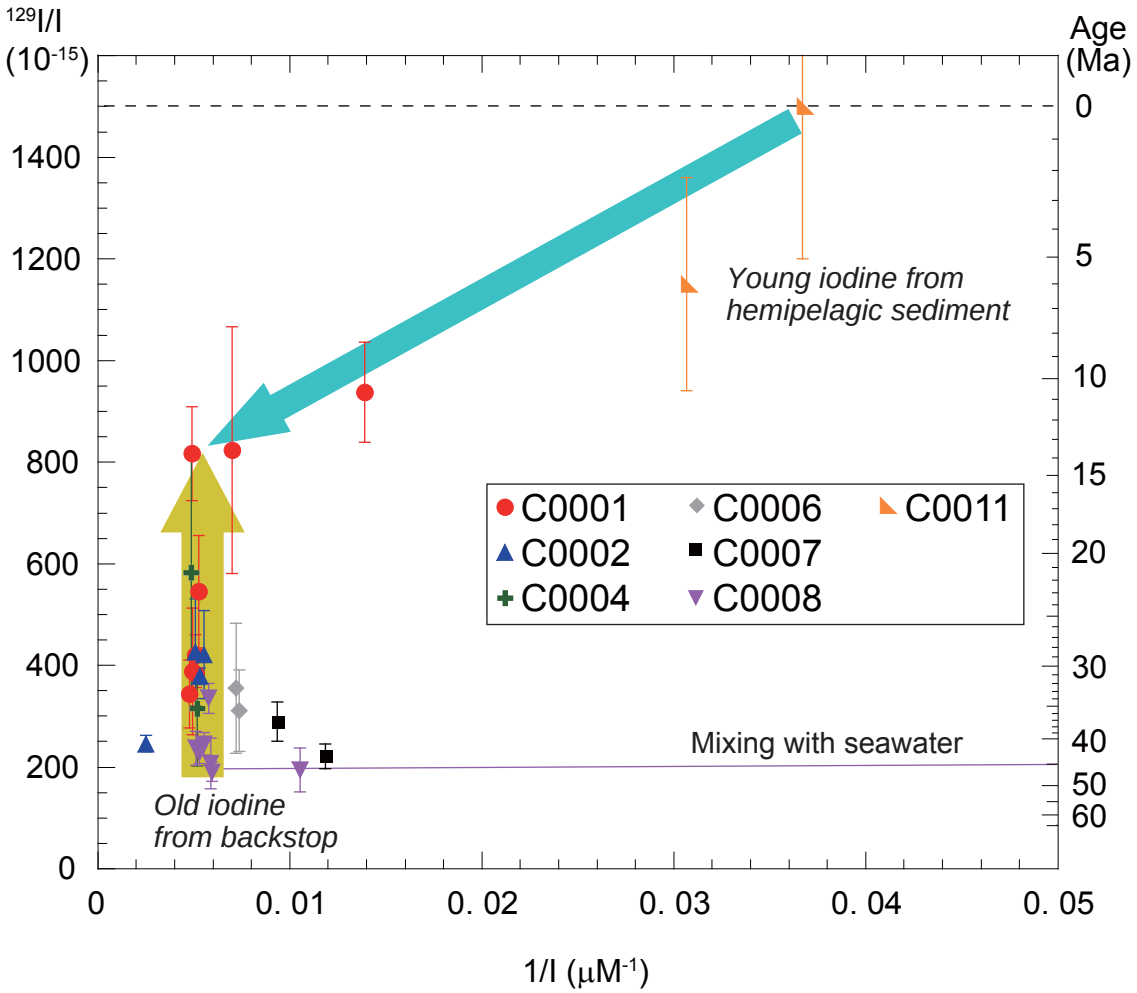
^{129}I/I
(10^{-15})
Age
(Ma)
1400
1200
1000
800
600
400
200
0
0
5
10
15
20
30
40
50
60
0
0. 01
0. 02
0. 03
0. 04
0. 05
1/I (μM^{-1})
Young iodine from
hemipelagic sediment
C0001
C0002
C0004
C0006
C0007
C0008
C0011
Mixing with seawater
Old iodine
from backstop

Fig.5

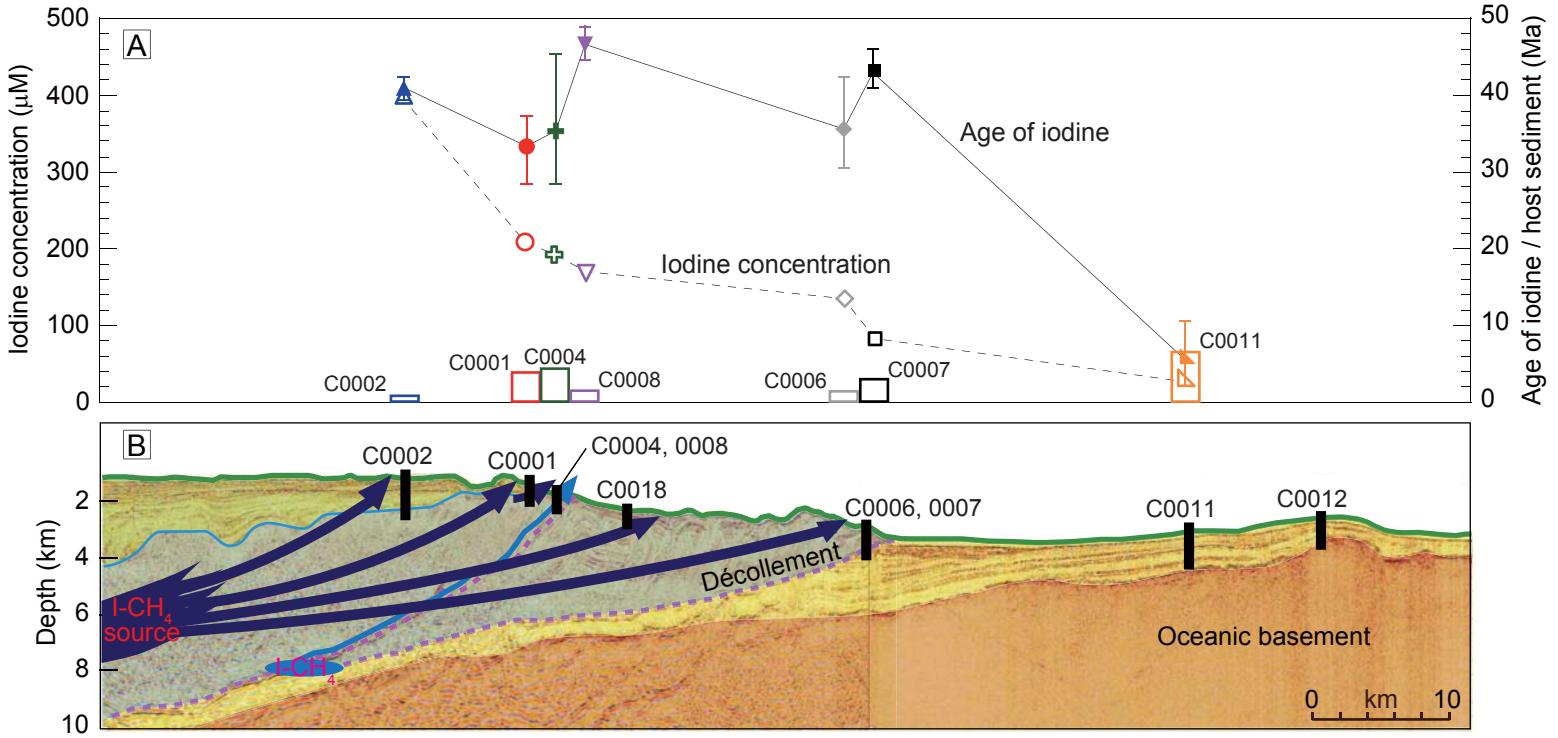
A
Iodine concentration (μM)
Age of iodine / host sediment (Ma)
Age of iodine
Iodine concentration
C0002
C0001
C0004
C0008
C0006
C0007
C0011
B
Depth (km)
C0002
C0001
C0004, 0008
C0018
C0006, 0007
C0011
C0012
Décollement
I-CH4 source
I-CH4
Oceanic basement
0 km 10

Fig.6